

## CHAPTER 13

### BEAM INSTRUMENTATION

#### 13.1 BEAM POSITION MEASUREMENT

A complete list of the beam position monitors associated with orbit and trajectory measurements is given in Tab. 13.1. There are three types of monitor: 24 mm button electrode monitors, 34 mm button electrode monitors and 120 mm stripline monitors. These are assembled in 13 different types of housing depending on the vacuum chamber dimension and interface with neighbouring equipment.

##### 13.1.1 Beam Position Monitors

The LHC orbit and trajectory measurement system has been developed to fulfil the functional specifications described in [1]. The system consists of 516 monitors per LHC ring, all measuring in both horizontal and vertical planes. The acquisition electronics is capable of 40 MHz bunch-by-bunch measurements and will provide closed orbit feedback at 1 Hz.

Table 13.1: List of beam position monitor types in LHC

Type	Electrode Type	Name	Number
Standard Arc	24mm Button	BPM	720
Dispersion suppressor & Q7	24mm Button	BPM	140
Standard BPM for vertical beam screen	24mm Button	BPMR	36
Enlarged Aperture BPM for horizontal beam screen	34mm Button	BPMYA	24
Enlarged Aperture BPM for vertical beam screen	34mm Button	BPMYB	12
Warm LHC BPM for MQWA	34mm Button	BPMW	36
Enlarged Warm LHC BPM for ADTV/H	34mm Button	BPMWA	8
Enlarged Warm LHC BPM for D2	34mm Button	BPMWB	16
Combined Button & Shorted Stripline BPMs	24mm Button + 150mm Stripline	BPMC	16
Cryogenic Directional Stripline Coupler for Q2	120mm Stripline	BPMS	8
Warm Directional Stripline Coupler for Q1	120mm Stripline	BPMSW	8
Warm Directional Stripline Coupler for D1	120mm Stripline	BPMSX	4
Warm Directional Stripline Coupler for DFBX	120mm Stripline	BPMSY	4
	TOTAL		1032

##### *Standard Arc Quadrupole Monitors*

The majority of the LHC beam position monitors (860 of the 1032) are of the arc type. These consist of four 24 mm diameter button electrode feedthroughs [2] mounted orthogonally in a 48 mm inner diameter beam pipe. The electrodes are curved to follow the beam pipe aperture and are retracted by 0.5 mm to protect the buttons from direct synchrotron radiation from the main bending magnets. Each electrode has a capacitance of  $7.6 \pm 0.6$  pF, giving a  $Z_{inf}$  of 1.4, and is connected to a 50  $\Omega$  coaxial, glass-ceramic, UHV feedthrough.

The button feedthroughs are connected to the cryostat feedthroughs via semi-rigid, 50  $\Omega$  coaxial cables capable of coping with cryogenic temperatures and high radiation environments [3]. These semi-rigid cables

are constructed from copper-clad stainless steel inner and outer conductors to give good electrical conductivity and poor thermal conductivity, and use a silicon dioxide foam dielectric. The N-type connectors on either end use a glass-ceramic dielectric seal. The cables work in a frequency range up to 2 GHz, with the electrical length difference in each quadruplet (the four cables associated with a BPM) being less than 10 ps.

The cryostat feedthrough will consist of four  $50\ \Omega$  ports with less than 4 ps electrical length difference between them and capable of resisting a high radiation environment [4].

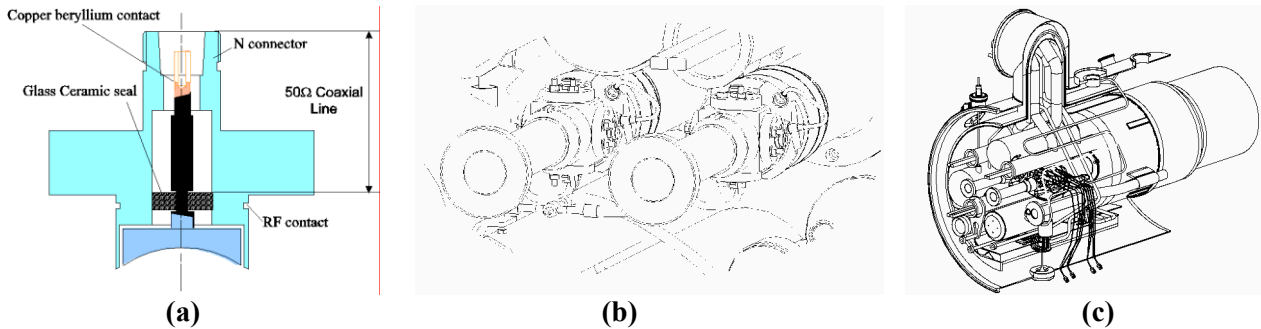


Figure 13.1: (a) 24 mm button electrode, (b) Mounted BPM bodies, (c) Location in the SSS cryostat including semi-rigid coaxial cables.

#### *Non-standard Insertion Region Monitors*

The inner triplet BPMs in all interaction regions are equipped with 120 mm,  $50\ \Omega$  directional stripline couplers (BPMS $\times$ ), capable of distinguishing between counter rotating beams in the same beam pipe. The location of these BPMs (in-front of Q1, in the Q2 cryostat and after Q3) was chosen as far as possible from a parasitic crossing to optimise the directivity. The 120 mm stripline length was chosen to give a signal similar to the button electrode, so allowing the use of the same acquisition electronics as for the arcs. The BPMs located in the Q2 cryostat is cold and rotated by  $45^\circ$  because of installation constraints. All cold directional couplers use an Ultem $\text{\textcircled{R}}$  dielectric for use in a cryogenic environment, while the warm couplers use a Macor $\text{\textcircled{R}}$  dielectric to allow bake-out to over  $200^\circ\text{C}$ .

The cleaning insertions in point 3 and 7 are equipped with warm, 34 mm diameter button electrode BPMs (BPMW) fitted either side of the MQWA magnets. The electrodes are an enlarged version of the arc BPM button described in section “*Standard Arc Quadrupole Monitors*”. Such button electrodes are also used for the cold BPMs in the matching sections either side of the four interaction regions as well as for the warm BPMs located near the D2 magnets and either side of the transverse damper (ADTV/H).

The BPMC, installed in point 4, are combined monitors consisting of one BPM using standard 24 mm button electrodes for use by the orbit system, and one BPM using 150 mm shorted stripline electrodes for use in the transverse damper system (see Chap. 6.4).

#### 13.1.2 Trajectory Acquisition System

The LHC orbit and trajectory acquisition system is based on a Wide Band Time Normaliser (WBTN) [5] capable of processing the analogue signals from the pick-up at 40MHz. The resulting signal is transmitted via a fibre-optic link, treated, digitised using a 10-bit ADC and processed by a VME64x Digital Acquisition Board (DAB) developed by TRIUMF, Canada [6].

#### *Front-end Chassis*

The front-end chassis for the majority of the LHC monitors will consist of four WBTN front-end cards, an intensity card and a WorldFIP control card. The chassis will be located below each SSS cryostat and is capable of processing the two planes from the BPMs of the counter rotating beams. The position information for each passing bunch is encoded in pulse width modulation using the wide band time normalisation principle [5] before being sent over a single mode fibre-optic link using a 2 mW, 1310 nm laser transmitter. In this way the radiation sensitive digital electronics can be separated from the more robust analogue electronics which will be subjected to 12 Gy or more per year during nominal LHC running.

The fibre-optic network linking the front-end electronics in the tunnel to the acquisition electronics located in surface buildings is comprised of ~125 km of ducting containing seven guide tubes. A mini-optical fibre-cable containing six or more fibres is blown into each guide tube and serves a single BPM front-end crate, leading to over 5000 km of installed fibre-optic links. A description of the characteristics and layout of the fibre-optic cabling can be found in Chap. 7 of Volume 2.

The intensity card installed in each chassis allows the simultaneous acquisition of both position and intensity (at the level of a few percent) for a single ring, with the intensity sent by the transmission system of the other ring.

The working mode, WBTN calibration and power supply surveillance of the front-end chassis is controlled via a WorldFIP receiver card using the single 31.25 kbit link serving each LHC sector.

For the insertion region BPMs the front-end chassis is located in neighbouring underground areas due to the high radiation doses around the BPM. In these cases highly phase-stable, ½ inch, 50 Ω, cellular polyethylene dielectric coaxial cable is used to connect the BPM electrodes to the front-end electronics.

### VME64x Acquisition Chassis

The VME64x acquisition chassis of the LHC orbit and trajectory system are located in the SR buildings at each access point. The chassis is comprised of a PowerPC, a TTC receiver (see Sec. 13.9) and up to 18 Digital Acquisition Boards (DABs), all linked via a custom AB/BDI VME64x backplane.

Each DAB is capable of processing the data from two WBTN mezzanine cards. A single WBTN mezzanine card receives treats and digitises the pulse modulated signal sent by a single front-end card, providing the DAB with a 40 MHz flow of 10-bit position data.

The DAB is capable of working in parallel in three different modes: orbit, capture (or trajectory) and post mortem. In orbit mode the incoming data is validated, calibrated and summed for 20 ms to eliminate 50 Hz noise. The result is retrieved by the PowerPC which calculates the average orbit for each plane and corrects the result for BPM geometrical non-linearity. This is repeated at 10 Hz, thus allowing the possibility of a 1 Hz closed loop orbit feedback. At the same time the incoming data is histogrammed to provide a standard deviation for each orbit reading.

In capture or trajectory mode the user is free to choose when, for which bunch(es) and for how many turns the DAB stores the position data, while the post-mortem mode stores the last 1000 orbits and 1000 turns in a circular buffer which is frozen by the beam abort system.

### 13.1.3 Expected Performance

The performance of the WBTN electronics with intensity is shown in Fig. 13.2. The system is expected to function with between  $2 \times 10^9$  and  $2 \times 10^{11}$  charges per bunch. A summary of the expected performance of the complete acquisition system for standard arc BPMs is presented in Tab. 13.2.

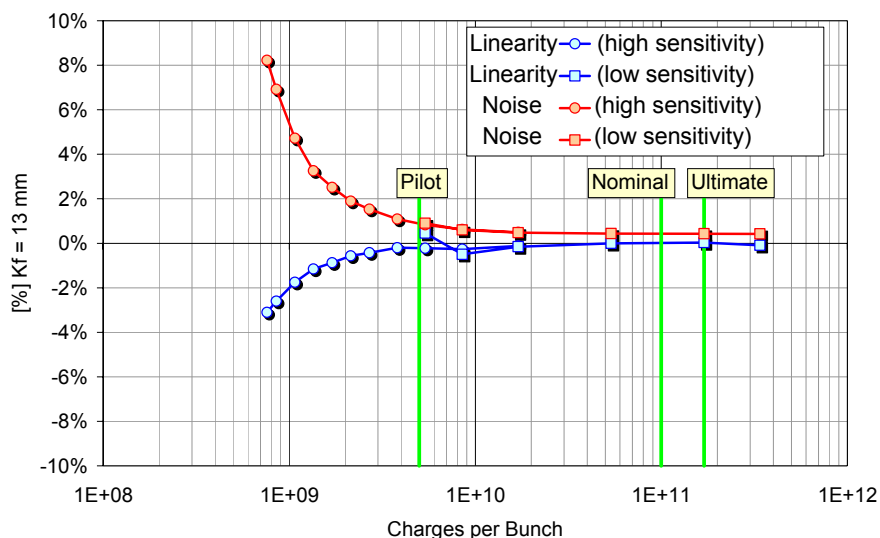


Figure 13.2: Performance of the LHC WBTN system with intensity.

Table 13.2: Expected performance of the LHC BPM system for standard arc BPMs

Range of Operation ( $\pm 6\text{mm}$ )	Pilot Bunch ( $5 \times 10^9$ )		Nominal Bunch ( $1.1 \times 10^{11}$ )		Ultimate Bunch ( $1.7 \times 10^{11}$ )	
	Single	Average over 224 turns	Single	Average over 224 turns	Single	Average over 224 turns
Resolution ( $\mu\text{m rms}$ )	130	9	50	5	50	5
Non-Linearity ( $\pm \mu\text{m}$ )	100					
Scale Error ( $\pm\%$ )	1					
Calibrator Offset ( $\pm \mu\text{m}$ )	50					
Intensity Offset ( $\pm \mu\text{m}$ )	25					
BPM & Gauge Mechanical Offset ( $\pm \mu\text{m}$ )	125					
Survey Measurement Precision ( $\mu\text{m rms}$ )	50					
Electrical Axis Offset ( $\pm \mu\text{m}$ )	113					
Uncertainty of MA wrt GA ( $\mu\text{m rms}$ )	150					
Geometric Non-Linearity ( $\pm \mu\text{m}$ )	100					
Total Offset ( $\pm \mu\text{m}$ )	363					
Relative Accuracy [offset ignored] ( $\pm \mu\text{m}$ )	302	155	183	154	183	154
Global Accuracy ( $\pm \mu\text{m}$ )	472	394	406	393	406	393

## 13.2 BEAM CURRENT TRANSFORMERS

Beam current transformers of two different kinds will provide intensity measurements for the beams circulating in the LHC rings as well as for the transfer lines from the SPS to LHC and from LHC to the dumps. The transformers will all be installed in sections where the vacuum chamber is at room temperature and where the beams are separated.

### 13.2.1 Fast Beam Transformers

The fast beam current transformers (FBCTs) will be capable of integrating the charge of each LHC bunch. This provides good accuracy for both bunch to bunch measurements and average measurements, intended mainly for low intensity beams for which the DCCT accuracy will be limited. For redundancy, two transformers with totally separated acquisition chains will be placed in each ring. These will be located in IR4. Each beam dump line will also be equipped with 2 redundant FBCTs, using the same acquisition electronics, for monitoring the ejected beam. In order to get good performance, there will be a dc restoration with a successive integrator and S/H circuitry used in the ring. The result of integration is digitized and stored in memory. Beam synchronous timing with 40 MHz frequency is used to trigger the system. The measurement precision for the pilot beam of  $5 \times 10^9$  protons in a single bunch is expected to be around 5 % (worst-case 10%), for the nominal beam below 1%. The transformer cores will use low droop, radiation hard material with a specified droop below  $2\%/\mu\text{s}$  and with the sensitivity approx. 1.25 V/A. Once injection is completed the transformers will be used to measure the circulating bunches by averaging the acquired bunch intensities over 20 ms yielding to approximate precision of 1% for pilot beam

### 13.2.2 DC Beam Transformers (BCTDC)

DC current transformers are based on the principle of magnetic amplifiers and will measure the mean intensity or current of the circulating beam and they can be used to measure the beam lifetime. Because of their operational importance, two of the devices will be installed in each ring. Currently a resolution of  $2 \mu\text{A}$  can be reached but a  $1 \mu\text{A}$  is targeted corresponding to  $5 \times 10^8$  circulating particles. The temperature dependence of the output current is  $\sim 5 \mu\text{A}$  per degree which makes either temperature stabilisation or frequent re-adjustment of the offset a necessity.

With an intensity of  $4.8 \times 10^{14}$  protons and a lifetime of 25 h driven by pp collisions the decay rate is  $5 \times 10^9$  protons/s. With a measurement time of 10 s this decay should be seen with 1% precision.

A resolution of  $1 \mu\text{A}$  is, however, insufficient for measurement of the pilot beam which can only be achieved with the fast transformers.

The front-end electronics generating the dc transformer feedback current should be placed as close as possible to the sensor in the ring. However, the radiation induced by the beam and by the RF cavities during their conditioning will be an issue. If the finest resolution is required for measuring the beam over the whole dynamic range, then an ADC of at least 20 bits, located in the front-end electronics is required. The data will be transmitted to the front end computer (DSC) installed in a surface building.

## 13.3 BEAM LOSS SYSTEM

### 13.3.1 Beam Loss Monitors

The loss of a very small fraction of the circulating beam may induce a quench of the super-conducting magnets or even physical damage to machine components. The detection of the lost beam protons allows protection of the equipment against quenches and damage by generating a beam dump trigger when the losses exceed thresholds. In addition to the quench prevention and damage protection, the loss detection allows the observation of local aperture restrictions, orbit distortion, beam oscillations and particle diffusion, etc. Since a repair of a superconducting magnet would cause a down time of several weeks, the protection against damage has highest priority.

#### *The measurement method*

The measurement principle is based on the energy deposition detection of secondary shower particles using ionisation chambers located outside of the magnet cryostats. The secondary particle energy flux is linear with the initiating protons parameters. To observe a representative fraction of the secondary particle flux detectors are placed at likely loss locations. The calibration of the damage and quench level thresholds with respect to the measured secondary particle energy deposition is simulation based.

#### *Dynamic range, resolution and response time*

The criteria used to define the dynamic range are given by the calculated damage and quench levels and the expected usage. The observation time range is defined by the fastest possible use of a beam dump trigger signal by the beam dump itself and the response time of the helium temperature measurement system.

Different families of BLM monitors are defined to ease the monitor design (see Tab. 13.3) [7].

Table 13.3: Functional families of BLM

<i>Type</i>	<i>Area of use</i>	<i>Dangerous consequences in the case of failures</i>	<i>Time resolution</i>
BLMC	Collimation sections	yes	1 turn
BLMS	Critical aperture limits or critical positions	yes	1 turn
BLMA	All along the rings	no	2.5 msec
BLMB	Primary collimators	no	1 turn bunch-by-bunch

There are basic criteria common to the BLMA, BLMS and BLMC:

- The high end of the dynamic range is set at three times the quench level. This takes into account the uncertainty of the evaluation of the quench level (factor of two). It also leaves a safety margin of a factor of nine (7.5) between the dump threshold and the high end of the BLM dynamic range at 450 GeV (7 TeV).
- The low end will be 5% of the quench level.
- For long integration times, the low end of the dynamic range is significantly reduced at 450 GeV to allow for extrapolation of the losses. The extrapolation from the pilot beam to the intermediate intensity beam requires a factor of 430 and an additional sensitivity factor of 10 is used.

### 13.3.2 BLMA

The dynamic range is specified in Fig. 13.3 and Tab. 13.4. The predicted quench levels depend on the loss duration and the beam energy. A continuous change of quench level thresholds is required during the beam energy ramp.

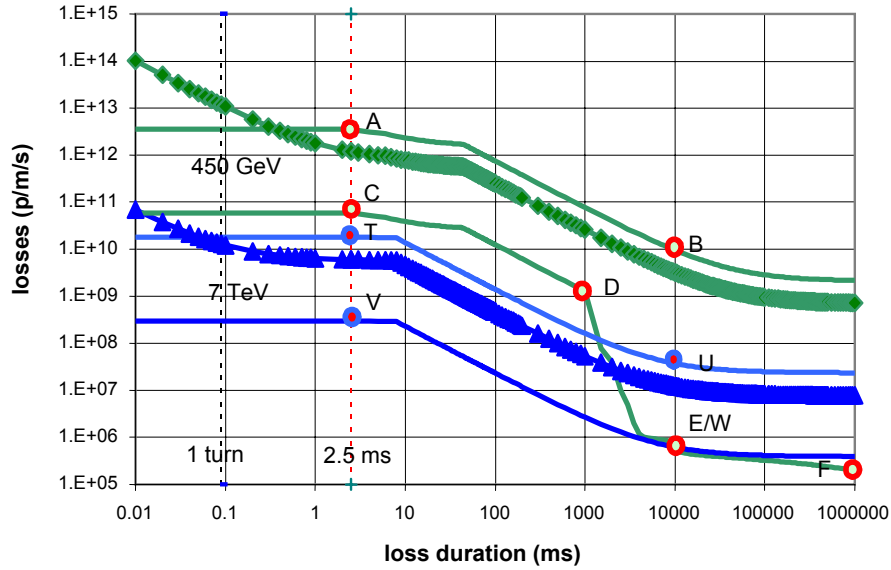


Figure 13.3: Quench levels as a function of the loss duration for the LHC arc bending magnet (marker + line) for 450 GeV (green squares) and for 7 TeV (blue triangles). The dynamic range is indicated by lines limiting either quench level curves. The loss rates marked by letters appear in Table 13.4, with their corresponding numerical values.

Table 13.4: Dynamic range for the BLMA and BLMS in units of Protons/m/s

	2.5 ms (BLMA) 0.1ms (BLMS)		1 s		10s		100s	
	<i>MIN</i>	<i>MAX</i>	<i>MIN</i>	<i>MAX</i>	<i>MIN</i>	<i>MAX</i>	<i>MIN</i>	<i>MAX</i>
450 GeV	$6 \times 10^{10}$ (C)	$3.6 \times 10^{12}$ (A)	$1.3 \times 10^9$ (D)		$8 \times 10^5$ (E)	$9.6 \times 10^9$ (B)	$2 \times 10^5$ (F)	
7 TeV	$3 \times 10^8$ (V)	$1.8 \times 10^{10}$ (T)			$6.25 \times 10^5$ (W)	$3.7 \times 10^7$ (U)		

### 13.3.3 BLMS

The BLMS has the same requirements as the BLMA, given in Fig. 13.3 and Tab. 13.3, except for their faster time response (1 turn, which corresponds to 89  $\mu$ s).

### 13.3.4 BLMC

The BLMC also have a time resolution corresponding to one turn. Their dynamic range must take into account the loss enhancement due to the collimation efficiency. This loss enhancement corresponds to a factor of between  $3 \times 10^3$  and  $1 \times 10^4$  (see Fig. 13.4).

Table 13.5: Dynamic range for the BLMC in units of Protons/s assuming a length of 1 meter.

	0.1 ms		1 s		10s		100s	
	<i>MIN</i>	<i>MAX</i>	<i>MIN</i>	<i>MAX</i>	<i>MIN</i>	<i>MAX</i>	<i>MIN</i>	<i>MAX</i>
450 GeV	$6 \times 10^{14}$ (C)	$3.6 \times 10^{17}$ (A)	$1.3 \times 10^{12}$ (D)		$4 \times 10^9$ (E)	$9.6 \times 10^{13}$ (B)	$1 \times 10^9$ (F)	
7 TeV	$6.5 \times 10^{11}$ (V)	$3.9 \times 10^{14}$ (T)			$6.25 \times 10^8$ (W)	$3.7 \times 10^{11}$ (U)		

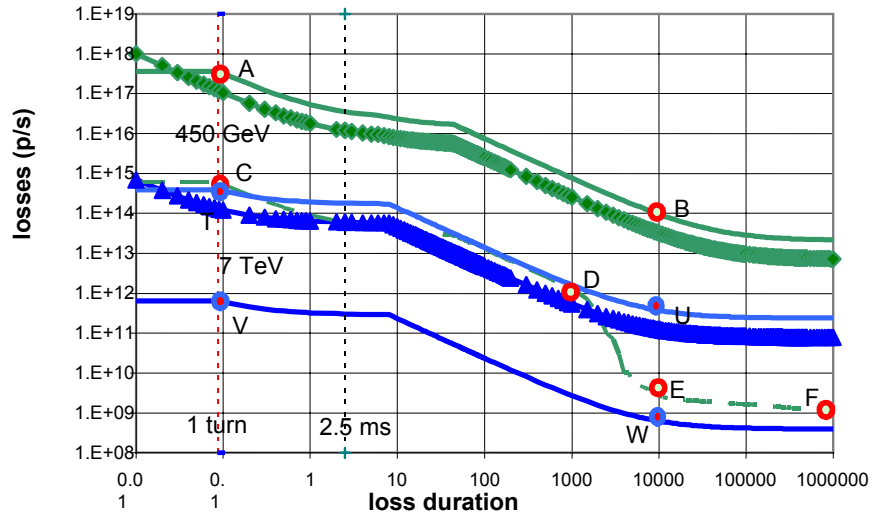


Figure 13.4: Total loss thresholds at all collimators (marker + line) for 450 GeV (green squares) and for 7 TeV (blue triangles) as function of the loss duration. The dynamic range for the BLMC is indicated by lines limiting either quench level curves. The loss rates marked by letters appear in Tab. 13.5, with their corresponding numerical values.

### 13.3.5 BLMB

The nominal functionality of the BLMB is to monitor any bunch-to-bunch variations. Their dynamic range is specified in Tab. 13.6.

Table 13.6: Dynamic range of BLMB

	<i>Lower limit</i>	<i>Upper limit</i>
BLMB	10% of the nominal steady losses at the collimators:	Warning level:
	$3.5 \times 10^6$ p/s per bunch (450 GeV)	$3.5 \times 10^8$ p/s per bunch (450 GeV)
	$1 \times 10^5$ p/s per bunch (7 TeV)	$7 \times 10^6$ p/s per bunch (7 TeV)

#### *Accuracy and reliability*

The damage and quench level prediction uncertainties are given by:

- Inaccuracy in the ionisation chamber particle flux measurements.
- Inaccuracy in the prediction of the secondary particle flux.
- Inaccuracy in the assumptions and predictions of the topology of proton particle loss distribution.
- Inaccuracy of the damage and quench level predictions.

Given the difference between the quench and damage levels of a factor of 5 at 450 GeV for loss duration larger as 10 s, the ultimate goal will be to calibrate the loss scale to within  $\pm 50\%$  (see Tab. 13.7).

Table 13.7: Precision of the detectors

Absolute accuracy (calibration)	< factor 2 (initial < factor 5)
Relative accuracy (to quench levels) for quench prevention	< $\pm 25\%$
Resolution for extrapolation	< quench level at 7 TeV/50

The target probability for magnet damage and the probability for a false dump are calculated using the SIL (Safety Integrity Level) approach [8]. The assumption of an LHC downtime period of 30 days as a consequence of magnet damage leads to a target probability for not detecting and dumping the beam in case of a dangerous loss of  $10^{-7}$  to  $10^{-8}$  per hour. A further analysis is required to determine if this low probability is required for every BLM channel.

The false dump probability of  $10^{-6}$  to  $10^{-7}$  is mainly driven by the assumption that ten unjustified dumps (dump requests from the system due to false triggers) could be accepted in one operational year.

### Secondary shower particles

Beam protons are likely to be lost at the location where the aperture is minimal: at 450 GeV this occurs at every arc quadrupole magnet and at 7 TeV at the triplet magnets. The beam loss monitors are located on either side of the magnets, in the horizontal plane defined by the beam vacuum tubes. Their longitudinal positions are about 1 m downstream of the most likely loss locations (see Fig. 13.5) [9, 10]. The centre of the quadrupole magnet and the bellows locations between quadrupole magnet and bending magnets are the anticipated loss locations. The optimisation of the location of the monitors is done using the criteria of maximum signal detection and the ability to distinguish between Beam 1 and Beam 2. A summary listing of the monitor locations is shown in Tab. 13.8.

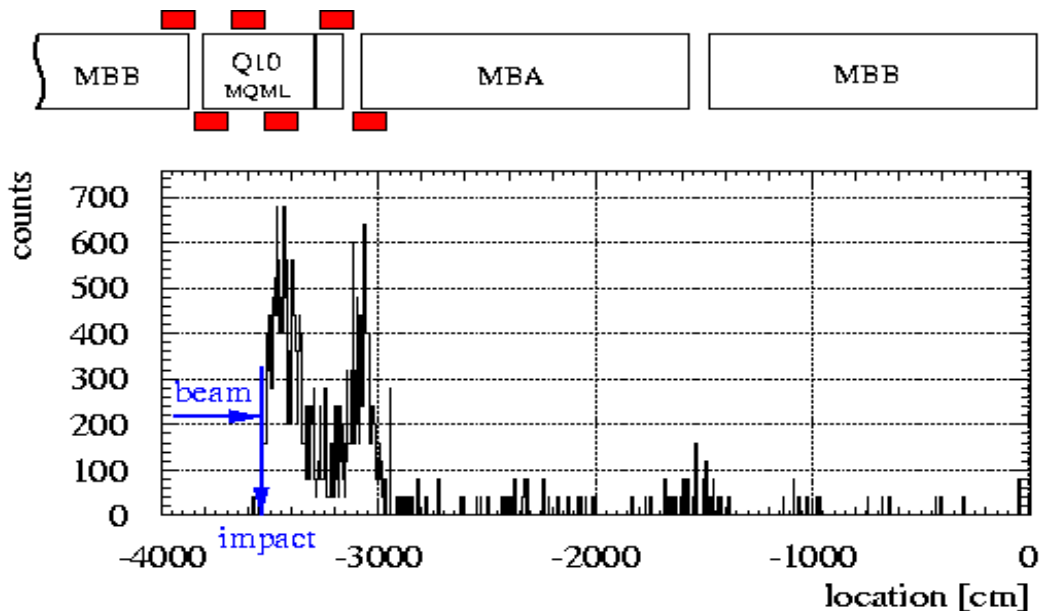


Figure 13.5: Scheme of the beam loss monitor locations in the vicinity of a quadrupole magnet (top). The simulated longitudinal particle shower distribution at the outside of the cryostat surface traversing a stripe with a height of  $\pm 5$  cm in respect to the horizontal plane (bottom) is shown. The initiating proton impact position is at the centre of the quadrupole magnet.

### The Monitor

The basic layout for the BLMA, BLMS and BLMC is shown in Fig. 13.6. The BLMB monitors are not yet defined.

The ionisation chamber signal is proportional to the energy loss of the traversing particles. The ionisation chamber has a volume of about 1 litre and the inner parallel electrodes are separated by 5 mm. The chamber is filled with  $N_2$  under normal pressure and a bias voltage of 1500 V is applied.

The chamber current for the BLMA and BLMS monitors varies between a few  $10^{-12}$  A and almost  $10^{-3}$  A. The BLMC ionisation chamber is not defined yet.



Table 13.8: Location and number of monitors.

	<i>Location</i>		<i>Number</i>	<i>Comments</i>
BLMC	IR3	1 primary, 6 secondaries	$7 \times 2$	At about 0.2 m downstream of each collimator
	IR7	4 primaries, 16 secondaries	$20 \times 2$	
BLMS	IR3	Cryobox DFBA	$2 \times 2$	Monitoring of the losses on the cryogenic feed-box
	IR7	Cryobox DFBA	$2 \times 2$	
	IR2,IR8	Septum MSI, Target TDI, TCDD, 2 collimators,D1	$6 \times 2$	Monitoring and protection against injection errors
	IR1, IR5	Absorbers: 2 TAS,	4	Monitoring of the losses at the TAS
	IR1,IR2, IR5, IR8	Triplets (2 per triplet) + BPM.Q1	$16 \times 2 \times 2$ $8 \times 2$	Maximum of beam size Exit of IP
	IR1, IR5	2 TAN absorbers, 4 experimental collimators	$12 \times 4$	Monitoring at the targets around the experiments
	IR6	Septum MSD, TCDQ, TCDS, DFBA	$4 \times 2$	Monitoring of the ejection to the dump channel
	DIS	MB adjacent to Q8 between Q7/Q8 + last MB before Q11, all DS's	$8 \times 4 \times 2$	Aperture limit in dispersion suppressors (momentum)
BLMA	LHC	At every quadrupole	$368 \times 2$	At the local maximum of the beam size
	movable		1	Movable goniometer covering a half-cell to be used in case of suspected aperture restriction
BLMB	IR7	At one primary collimator per plane	$2 \times 2$	Monitoring of the losses at 40 MHz

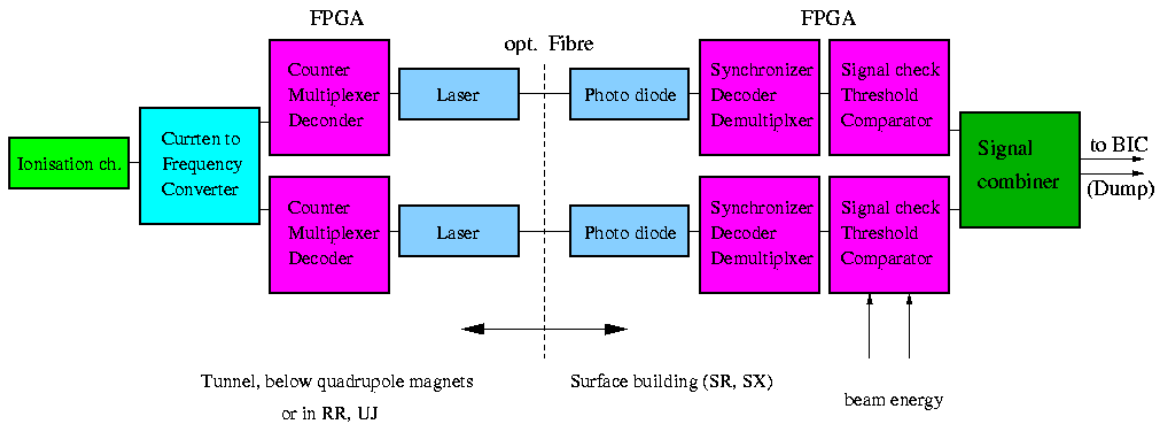


Figure 13.6: The schematic view of the ionisation chamber signal transmission and treatment chain.

The cable length between chamber and front end electronics (BLMCFC) varies between 10 m for the BLMA (below quadrupole magnets) and maximum 400 m for the BLMS (RR and UJ locations). The chamber current is converted to a corresponding frequency and these pulses are counted over a period of 40  $\mu$ s. The counter value is transmitted every 40  $\mu$ s to the surface analysis electronics (BLMTC) using a

dedicated fibre link. The BLMTTC compares the measured loss values with the loss duration and energy depending threshold values. The warning information is transmitted by a software protocol and the dump signals are transmitted to the dump kicker magnets using the beam interlock controller (BIC). The energy information is received over a dedicated redundant fibre link. The signal treatment and transmission chain is redundant after the current to frequency conversion to meet the required dangerous consequence probability of  $10^{-7}$  to  $10^{-8}$  per hour.

### 13.4 TRANSVERSE PROFILE MEASUREMENT

The analysis of the anticipated uses allows the definition of four functional modes to be mapped on the different types of hardware monitors:

- A single-pass monitor of high sensitivity (pilot beam) with a modest demand on accuracy and few restrictions on the beam blow-up due to the traversal.
- A “few-pass monitor” (typically 20 turns) dedicated for the intermediate to nominal intensity range of the injected beam for calibration or matching studies. The blow-up per turn should be small as compared to the effect to be measured.
- A circulating beam monitor, working over the whole intensity range. No blow-up is expected from such a monitor.
- A circulating beam tail monitor optimised to scan low beam densities. In this mode one may not be able to measure the core of the beam. The measurement should not disturb the tail density significantly.

IR4 is the default location for all instrumentation.

#### 13.4.1 Single Pass Monitors

Five monitors are planned at each injection point into LHC, and an extra monitor will be installed between quadrupoles Q6 and Q7 at the exit of the first arc after injection. Its location is in the middle of the drift where both the H and V amplitude functions have same value (about 100 m), thus providing equal beam size in either plane. The position of the single-pass-monitors in each LHC ring is summarised in Tab. 13.9.

Table 13.9: Layout of single-pass monitors

Entry septum MSI
Exit septum MSI
Entry kicker MKI
Exit Kicker MKI
Entrance TDI absorber
Between Q6 and Q7
in LSS3 left (for Ring1 and Ring2, also needed for matching studies)
in LSS7 right for Ring2
Between Q5 and Q6 in LSS4 for Ring1 & Ring2 (used also for matching studies)

#### 13.4.2 Few-pass Matching Monitors

For matching studies at injection a matching monitor is needed in each ring at a position where the dispersion is significant ( $> 1$  m) and the horizontal and vertical beam sizes are both large enough to offer the best sensitivity, i.e. in the middle of a drift. The nominal matching monitor will be installed in IR3 between Q6 and Q7 (Tab. 13.9). Optional matching monitors (dispersion free) can be installed in IR4 between quadrupoles Q5 and Q6 (Tab. 13.9 and Fig. 13.7), where rms values of 1.25 mm at 450 GeV will be measured. Another application of these monitors would be first turn observation during injection studies (Tab. 13.9).

### 13.4.3 Circulating Beam and Tail Monitors

For the best performance, this type of monitor should be placed at large  $\beta$ -values. In addition, with a  $\beta$ -ratio of 2 or more between planes, the tilt due to the coupling of a round beam becomes observable. The following positions have been selected and fulfil the requirements both for the baseline program and for extensions allowing more precise monitors if the need arises:

#### *IR4 synchrotron light monitor*

In each ring a synchrotron radiation monitor is under development, using a signal provided by superconducting (SC) undulators installed upstream of the D3 separator magnet, as shown in Fig. 13.7. Profiting from the beam deflection generated by D3, the light is extracted 10 m downstream of D3, providing a two dimensional transverse image of the beam.

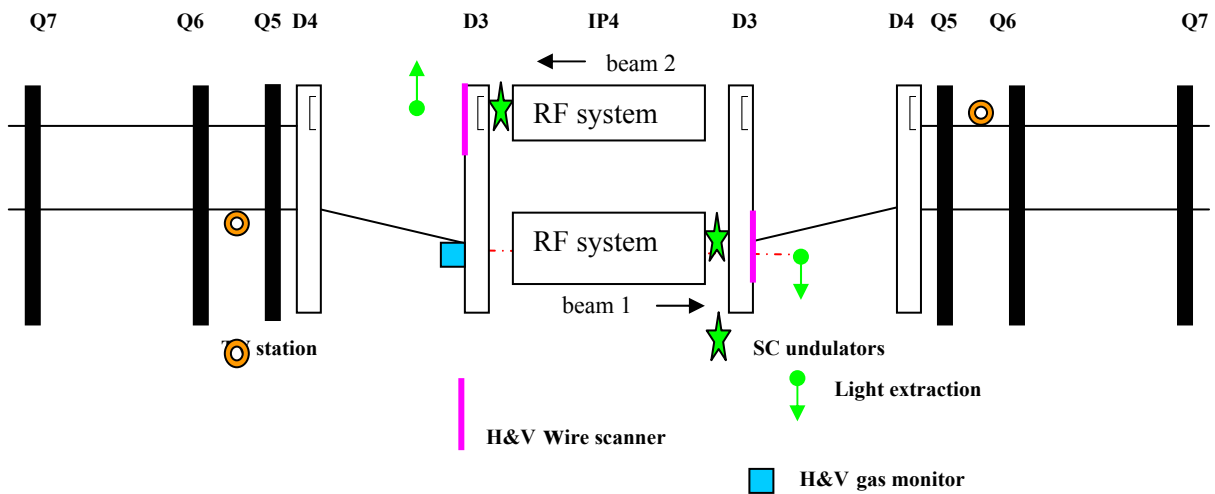


Figure 13.7: Configuration of transverse profile monitors in IR4.

#### *IR5 synchrotron light monitor*

This location will be kept as an option. It provides the best resolution for flat top energy operation on the collision optics, with local amplitude functions of 590 m and 1600 m, respectively, in the horizontal and in the vertical planes. The monitor uses the light emitted by the beam within the magnet D2, which is extracted 20 m later. The setup here is shown schematically in Fig. 13.8.

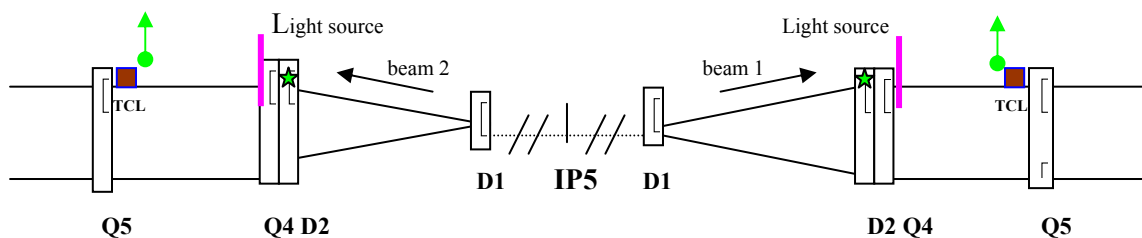


Figure 13.8: Telescope configuration in IR5.

#### *IR4 Gas monitors*

Gas monitors, exploiting either the rest gas ionisation signal or looking at the luminescence light resulting from de-excitation of the gas atoms, are being considered. For each beam one monitor with good resolution in each transverse plane is required. A location close to D3 is favourable, where the separation between the beams is largest and where the amplitude functions are close to 250 m. These locations are shown on Fig. 13.7.

Table 13.10: Accuracy and resolution necessary

Mode		Beam scenario	Observation mode	Precision
Single-pass to Few-pass	Beam spot	1 pilot to 1 nominal SPS batch	Turn-by-turn	Accuracy: <ul style="list-style-type: none"> <li>• 20% rms on <math>\sigma</math></li> <li>• average position: <math>\approx 300 \mu\text{m}</math> rms</li> </ul>
	matching	1 intermediate bunch to SPS batch	Turn-by-turn over 20 turns	Resolution: $\pm 20\%$ on $\sigma$
Intermediate to ultimate SPS batch				
Circulating	beam size and profile	Pilot to intermediate beam	$10^3$ turns	Resolution: 10% rms on beam $\sigma$
		intermediate to ultimate beam		Resolution: <ul style="list-style-type: none"> <li>• 1% rms on beam <math>\sigma</math></li> <li>• 5% rms on bunch <math>\sigma</math></li> <li>• 10% rms on transv. distribution points</li> <li>• (<math>\pm \sigma/10</math> in beam position)</li> </ul>
			$10^2$ turns	Resolution: 5% rms on beam $\sigma$
	Beam emittance		$10^3$ turns	Accuracy: $\pm 5\%$ on beam $\sigma$
	tail	intermediate to ultimate beam	$10^4$ turns	Resolution: 10% rms on transv. distribution points
	dynamic aperture	1 pilot to one intermediate bunch	$10^3$ to $10^4$ turns	Resolution: $\pm 10\%$ on transv. distribution points
	calibration	Pilot bunch to nominal PS batch	No constraint	Accuracy: 1% rms on $\sigma$

#### IR4/IR5 Wire scanners

Wire scanners will be installed in IR4. Their position is illustrated schematically in Fig. 13.7. They will be used principally for absolute calibration of the other monitors, but also as tail monitors. Their use for calibration purposes imposes the most demanding accuracy; typically 1%. To overcome uncertainties related to  $\beta$ -beating, they would ideally be at the same location as the SC undulators or the other emittance monitors. However, in order to minimise the risk of quenching the D3 magnet when they are used, they will be installed immediately downstream of this magnet as shown in Fig. 13.7. The installation of a Synchrotron Light telescope in IR5, would also be complemented by the installation of wire scanners (Fig. 13.8) for the absolute calibration.

The accuracy and resolution to be achieved in the various modes is summarised in Tab. 13.10.

### 13.5 LONGITUDINAL PROFILE MEASUREMENT

This instrument profits from the Transverse Profile Monitor light source [11] with the aim of using synchrotron light to measure bunch profiles with a dynamic range of  $10^5$ , enabling measurements and monitoring of bunch lengths, tails, un-bunched beam, ghost bunches and the abort kicker rise time gap.

A part of the synchrotron light generated by the superconducting bending and undulator magnets of the Transverse Profile Monitor is collected by a separate fixed mirror offset behind the transverse optics. It is estimated [12] that  $2 \times 10^6$  photons will be collected per passage of each  $1.1 \times 10^{11}$  proton bunch; this intensity remains reasonably constant from injection energy up to 7 TeV. However, the spectral distribution changes with beam energy, at injection energy the undulator produces a distribution peaked around 950 nm but at

higher energies the spectral profile is from 200 nm to 2000 nm, although only a part of this range can be used by the instrument.

The photon flux reliably mimics the beam in both time and intensity, the specification [13] calls for the photons to be detected with 50 ps precision: two detection methods are under study at Lawrence Berkeley Lab, who will produce the instrument as part of the LARP collaboration. One possible system is to use a laser oscillator which generates  $\sim 20$  ps pulses at a high repetition rate (40 MHz), synchronised to sample the entire LHC rotation at 50 ps intervals. The synchrotron light can be mixed with a laser pulse, the amplitude of the resulting wavelength-shifted pulse can then be measured by a fast detector, and data is then accumulated in registers to build up the required data profiles. A prototype Laser-Mixing (LM) system has been successfully used to measure beam profiles at the Advanced Light Source at LBNL.

An alternative system is to use an array of fast Single Photon Detectors (SPD) and time-of-flight recorders, continuously detecting the photon flux with the data being accumulated into registers as before. A decision on the best system for LHC will be made in 2004.

The need to sample the entire LHC circumference with 50 ps intervals would lead to 2 million data bins: a serious data handling task. This can be minimised by coding each sample point with the relevant measurements: for example, of the  $\sim 35,500$  RF buckets, only 2808 should contain bunches, so the data from the majority of sample points will accumulate into the measurement of ghost bunch current or debunched beam.

At injection energy the LPM will monitor the intensity of the debunched beam to ensure safe conditions before the acceleration ramp starts, the maximum safe level being 1500 times lower than the nominal bunch intensity. It is also necessary to ensure that the abort kicker rise time gap remains empty; here the 3  $\mu$ s gap is divided into 30 measurement bins of 100 ns length.

Individual bunches, groups of bunches, or the entire fill can be targeted to provide the bunch centre of gravity, length, core distribution and distribution in the low intensity tails, the sensitivity and range of the measurements will depend on the integration time available. An absolute intensity calibration can be made by comparing the total integrated beam intensity with a beam current monitor.

## 13.6 LUMINOSITY MONITORS

### 13.6.1 Introduction

The nominal LHC luminosity for IR1 (ATLAS) and IR5 (CMS) is  $10^{34}$   $\text{cm}^{-2}\text{s}^{-1}$ , for beams of 2808 bunches of  $1.1 \times 10^{11}$  protons each. The other two interaction regions will have lower nominal luminosities of the order of  $10^{32}$   $\text{cm}^{-2}$   $\text{s}^{-1}$  for IR8 (LHCb) and  $10^{30}$   $\text{cm}^{-2}\text{s}^{-1}$  for (IR2) ALICE. With different filling patterns and optics, the global range of luminosities goes from  $10^{26}$  to  $10^{34}$   $\text{cm}^{-2}\text{s}^{-1}$  and for the ion runs between  $10^{24}$   $\text{cm}^{-2}\text{s}^{-1}$  and  $10^{27}$   $\text{cm}^{-2}\text{s}^{-1}$ .

The proton beams are bunched with a bunch-to-bunch distance of 25 ns (or a multiple of 25 ns). This corresponds to a maximum bunch crossing frequency of 40 MHz. In nominal conditions the beams do not collide head on, but with a small angle of the order of 150-200  $\mu$ rad to avoid unwanted collisions near the IP. The plane containing the two beams (collision plane) can be rotated and be different in the four interaction regions.

### 13.6.2 Machine Requirements

The aim of the machine luminosity monitors [14] is to measure the interaction rates for the setup, the optimisation and the equalisation of the beams at the interaction regions. For this purpose they must be simple, fast and robust and preferably be of one design for all four IR's. These instruments are required to measure the interaction rate with a good relative accuracy; the absolute value can be obtained with frequent cross calibrations with the luminosity monitors installed in the experiments, or other methods. The calibration factor must remain stable over a reasonable amount of time and must not be influenced by the machine parameters (steering, optics etc.)

The requirements on the accuracy go from around 10% for the beam finding mode to 0.25 % for the collision feedback. Measurement times also vary from minutes in beam finding mode (very low luminosity) to one second at nominal luminosity. The monitors should also allow the measurement of the crossing angle with accuracy better than 10  $\mu$ rad in the range 0-200  $\mu$ rad.

In order to detect and correct eventual bunch-by-bunch effects the bunch-by-bunch luminosity measurement is required. The detectors, readout and acquisition systems must thus be capable of operating with a useful bandwidth of 40 MHz. The bunch-by-bunch measurements, the average luminosity and crossing angle should be sent to the main control room and also dispatched to the experiments.

### 13.6.3 Instrument Description

The machine luminosity monitors are in fact flux monitors. They are installed in the TAN absorbers 141 m away on both sides of the high luminosity IR's (1 & 5) and equivalent positions in IR2 and IR8. They measure the flux of the showers generated by the neutral particles created in the collisions (neutrons and photons). Neutral particles are chosen in order to suppress the background related to beam losses. The radiation dose to the detectors is very large, 170 MGy/yr, and poses a constraint on the choice of the technology.

The detectors have a rectangular surface  $\sim 10 \text{ cm} \times 10 \text{ cm}$ . Each detector consists of four rectangular fast, pressurised, gas ionisation chambers, assembled in a  $2 \times 2$  array, and are placed behind  $\sim 30 \text{ cm}$  of copper at the shower maximum inside the TAN [15].

An alternative technology still under investigation consists of the use of polycrystalline CdTe discs in a  $2 \times 5$  array. This solution offers a better sensitivity, time resolution and angle measurement. The radiation hardness of this type of technology is however still under investigation.

In both cases the signals have to be transported using radiation resistant cables to a less radioactive area behind the TAN where the first stage of the electronic system is installed and then from there sent to the counting room where they will be acquired using the DAB (Digital Acquisition Board) developed at the TRIUMF Laboratory for the orbit measurement system.

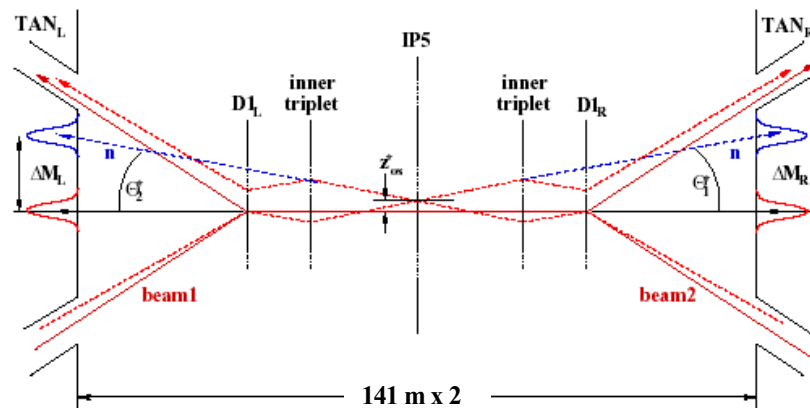


Figure 13.9: Schematic layout of the interaction region at IP5 (CMS).

## 13.7 TUNE, CHROMATICITY, AND BETATRON COUPLING

The reliable measurement of betatron tune,  $Q$  (and the related quantities tune-spread, chromaticity and betatron coupling), will be essential for all phases of LHC running from commissioning through to ultimate performance luminosity runs. For injection and ramping, the fractional part of the betatron tune must be controlled to  $\pm 0.003$ , while in collision the required tolerance shrinks to  $\pm 0.001$ . With the exception of Schottky scans (see Sec. 13.9) and the “AC-dipole” excitation outside the tune peak (Sec 13.10), all  $Q$  measurement techniques involve some disturbance to the beam. The resulting emittance increase, while acceptable for some modes of running, e.g. with pilot bunches, will have to be strongly limited for full intensity physics runs. Two distinct tune measurement systems are therefore envisaged, as described below.

### 13.7.1 General tune Measurement System

This system will allow the measurement of tune via standard excitation sources (single kick, chirp, slow swept frequency, and noise). It should operate with all filling patterns and bunch intensities and be commissioned early after the LHC start-up. Even with oscillation amplitudes down to  $50 \mu\text{m}$ , a certain

amount of emittance increase will result, limiting the frequency at which measurements can be made. It will therefore probably be unsuitable for generating measurements for an online tune feedback system.

### *Detectors*

Dedicated stripline couplers will be mounted on 2-3 m long motorised supports that can be displaced horizontally or vertically with a resolution of 1 or 2 microns. There will be two such supports near Q6 and Q5 left of IR4 and another two at Q5 and Q6 right of IR4. They will measure in one plane only to profit from the high  $\beta_h$  or  $\beta_v$  near each quadrupole (typically 400 m). Also mounted on each support will be the resonant pick-up (see Sec. 13.7.3) and a standard warm button BPM dedicated to providing positions for a slow feedback loop keeping the BPM centred about the beam. This will allow the electrical aperture of the tune coupler to be reduced to measure small position deviations about the closed orbit. Also, taking into account the higher signal level from the coupler design, the dedicated tune pick-ups will have a much higher sensitivity than the normal closed orbit BPMs for transverse oscillation measurements. If necessary, electronic common mode rejection could also be included in the processing chain. Measurements of individual bunch positions have been requested for this system.

When the oscillation amplitude is sufficiently large, the orbit BPMs can also be used for tune measurement. It will be possible to measure the betatron function and phase advance all around the ring with them.

### *Kickers*

Four kicker magnets will be installed around IR6 (one for each plane and each beam) to excite coherent oscillations of part of the beam with a short kick pulse. The current specification calls for a Q-kick generator producing 9  $\mu$ s base half-sine pulses with a superimposed 3<sup>rd</sup> harmonic to make the pulse more square. The length has been optimised to kick 3 x 72 bunches, with limited disturbance of the neighbouring batch. The maximum oscillation amplitude produced corresponds to  $2.6\sigma_T$  at 450 GeV and  $0.7\sigma_T$  at 7 TeV. A kick repetition rate of 1 Hz should be possible. The minimum kick available at 450 GeV will be 50  $\mu$ m. The kicker magnets (identical to a dump-kicker module) will also be driven by a more powerful “aperture” generator producing an 89  $\mu$ s base half-sine pulse corresponding to up to  $8\sigma_T$  at 7 GeV.

An alternative scheme using only one generator per magnet with a maximum kick of  $6\sigma_T$  at 450 GeV and  $1.7\sigma_T$  at TeV is presently under study. If accepted, this would facilitate kick-based Q measurement at 450 GeV and 7 TeV and the exploration of the dynamical aperture at only 450 GeV. If an  $8\sigma_T$  kicker were really required at 7 TeV, then this could be retro-fitted in about one year, once the LHC start-up has taken place. The disadvantage for Q measurement is that three times more beam is kicked at a time and so, on a completely filled machine, fewer kicks would produce a given emittance increase of the whole beam.

### *Use of transverse feedback kickers*

The general tune measurement system will make use of the transverse feedback kickers, as is done in the SPS. Reducing the feedback gain in unstable beam conditions, and injecting noise, chirps (fast frequency sweep), or slow swept frequency are all possibilities that can be exploited for tune measurement. Cabling and patch panels for introducing signals into the feedback loops in SR4 and also in UX45 have been planned.

It is clear that there exists a certain incompatibility between transverse feedback and precision tune measurement: namely that the damping action will broaden the tune resonance to an extent precluding the desired precision of 0.001 of the tune measurement. It is to be hoped that short intervals (some 10<sup>3</sup>s of ms) with reduced feedback gain can be tolerated while a tune measurement is made. An alternative approach using frequencies near the top limit of the transverse feedback bandwidth is described in the next section.

## 13.7.2 AC Dipole

### *Principle of the AC-dipole excitation*

The emittance-conserving beam excitation was studied at BNL for adiabatic resonance crossing with polarised hadron beams. It was realised that the same principle can be used to diagnose the linear and non-linear transverse beam dynamics.

The principle is as follows: the beam is excited coherently at a frequency close but outside its eigenfrequencies by an oscillating dipole field. Hence the name AC dipole is given to the exciter. In the simplified model of a linear oscillator, the beam is expected to oscillate at the exciter frequency with a phase shift of  $\pi/2$ . The energy of the coherent oscillation does not couple with the incoherent oscillations of the individual beam particles. There is therefore no change of beam emittance.

It is important to note that the forced beam oscillation amplitude is inversely proportional to the difference of the betatron tune and the exciter frequency, which is the major parameter in the design of the AC-dipole force:

- One would like to create big oscillation amplitudes, which demand the excitation frequency to approach the betatron tune.
- One wants to preserve beam emittance, which in practice demands a minimum difference between exciter frequency and betatron tune of about  $0.02 * f_{ref}$ .

More details in particular on the excitation scheme can be found in [16] and in the references therein.

#### *Requirements of an AC-dipole for the LHC*

At present, the functional specifications for an AC-dipole beam excitation are not complete. The following issues are clear:

- Accelerator physicists would like to use this tool in order to excite sizable beam oscillations at 7 TeV beam energy for diagnostics purposes (several sigma).
- For such extreme cases the minimum frequency difference between exciter and betatron tune could be chosen smaller and one would expect some beam blow-up.
- One has to be able to change the frequency of the AC-dipole by about 10% in order to adapt to changes of the machine tunes.
- An AC dipole excitation for both planes and both rings is requested.

#### *Technical solutions*

No work has so far been invested in a detailed design and therefore only a few things can be listed:

- The exciter frequency will be around 3 kHz, which precludes a superconducting magnet or a steel magnet. The skin effect is not yet very important at that frequency, such that an air core magnet with cosine density distribution of the windings can be envisaged.
- By adding a parallel capacitor to the magnet winding a resonant circuit will be created, which will be driven by a power amplifier. The time envelope of the excitation will be created in the low power part driving the amplifier.
- First estimates [17] of the power necessary show an enormous reactive power of more than 10 MVA needed in the AC-dipole, if the requirements on the kick strength are maintained. This value is for a magnet of about 10 m length.
- It is very difficult to achieve a 10 % tunability of such a high power device. Movable ferrite blocks to change the inductance of the coil have been studied at RHIC, but have not been realized. DC polarisation of the coil ferrite material is possible, but will require huge dc currents. As an alternative, the use of a second amplifier, which will act as variable capacitance in a circuit called “gyrator” is being studied.

### 13.7.3 High Sensitivity Tune Measurement System

The beam is excited by applying a signal of low amplitude and high frequency,  $f_{ex}$ , to a stripline kicker.  $f_{ex}$  is close to half the bunch spacing frequency,  $f_b$ , (for the nominal 25 ns bunch spacing  $f_b = 40$  MHz). The equivalent oscillation amplitude should be a few micrometers or less at a  $\beta$ -function of about 200 m. A notch filter in the transverse feedback loop suppresses the loop gain at this frequency, where instabilities are not expected to be a problem. If the excitation frequency divided by the revolution frequency corresponds to an integer plus the fractional part of the tune then coherent betatron oscillations of each bunch build up turn by turn (resonant excitation).



A batch structure with a bunch every 25 ns “carries” the frequency  $f_{ex}$  as sidebands of the bunch spacing harmonics (i.e. at  $(N \times 40 \text{ MHz}) \pm f_{ex}$ ). A beam position pick-up is tuned to resonate at one of these frequencies. By linking the generation of the excitation signal and the processing of the pick-up signal in a phase-locked loop (PLL) feedback circuit, the excitation can be kept resonant and the tune can be determined continuously. Emittance growth is controlled by maintaining the excitation level as small as possible, compatible with the required measurement precision and rate. Since the first derivative of the phase as a function of frequency goes through a maximum at the central value of the tune, this method gives the highest precision for a given oscillation amplitude. The tune values produced could be used as input to a tune feedback loop.

It must be emphasized though that the present design of the system is optimised for luminosity runs with batched beams with 25 ns bunch spacing. The handling of other bunch spacings at multiples of 25 ns should be possible, but the magnitude of the pick-up signal diminishes with increasing bunch spacing.

The development of a PLL tune measurement system for the LHC is being done in collaboration with Brookhaven National Laboratory, where a similar system has been installed in RHIC. It is clear that the system will not be operational during the early stages of commissioning the LHC. Indeed, the beams planned for initial commissioning (single bunch, 43 equally spaced bunches, etc.) are incompatible with this method.

#### 13.7.4 Chromaticity Measurement

At injection it is expected that the linear chromaticity must be controlled to better than  $\Delta Q' = \pm 1$  unit. This relaxes to  $\pm 3$  units in collision. During the “snap-back” phase of the magnet cycle at the beginning of the ramp the  $b_3$  multipole in the main dipoles can generate a chromaticity change of up to 2.7 units per second. Feed-forward, on-line reference magnet measurements and modelling should reduce this rate, but not to zero. At the time of writing there is no proven chromaticity measurement system that can produce data for a feedback loop at these rates for full intensity physics beams.

##### *Energy modulation*

Since chromaticity is proportional to the rate of variation of tune with beam energy, the classical measurement method consists of varying the beam momentum and measuring the induced change in betatron tune. The beam momentum is most conveniently changed by modulating the RF frequency. The drawbacks for use in the LHC are the relatively slow rate of RF frequency modulation (of the order of 0.1 Hz) and the magnitude of the consequent orbit changes. The method will be available for machine setting up, but is incompatible with normal operation.

A promising alternative method of modulating the energy that has been proposed recently is fast RF phase modulation. In the LHC, a  $3^\circ$  RF phase change seems feasible, corresponding to  $\Delta E/E$  of  $5 \times 10^{-5}$ . The modulation rate must be significantly higher than the synchrotron frequency (20-60 Hz in the LHC). Experiments are under way in the SPS [18]. Unlike the head-tail method described below, this method does not suffer from the problem of producing an excessive emittance increase.

##### *Head-tail phase shift measurements*

The so-called "Head-Tail" chromaticity measurement allows the chromaticity to be calculated from several hundred turns of data after a transverse kick. The measurement relies on the periodic de-phasing and re-phasing that occurs between the head and tail of a single bunch for non-zero chromaticity. By measuring turn-by-turn position data from two longitudinal positions in a bunch it is possible to extract the relative de-phasing of the head and the tail, and so to determine the chromaticity.

Couplers with striplines sufficiently long to allow separation of the principal and reflected beam pulses ( $\sim 50$  cm) will be installed on motorised supports near Q5 and Q6 left of IP4. As for the tune pick-ups, a slow position feedback will keep the detectors centred on the beam, maximising the precision of the oscillation measurements. The beam signals will be digitised with fast ADCs sampling at 2 Gs/s or more, with analogue bandwidth above 1 GHz.

A system has been installed in the SPS and encouraging results obtained [19]. However, although the measurement can be repeated at a reasonable rate (0.5 Hz has been obtained, but a faster rate is possible), the use of oscillations in the mm range would probably produce an unacceptably large emittance increase on beams for physics. This instrument seems best suited for producing feed-forward type corrections.

### 13.7.5 Betatron Coupling Measurement

The working point of the LHC will be very close to the diagonal, so that insufficient compensation of the betatron coupling will make tune and chromaticity measurement very difficult. Two classical methods that can be used to measure betatron coupling are the closest tune approach and the kick method. In the former method, both betatron tunes are measured continuously during a linear power converter ramp that crosses the values of the horizontal and vertical tunes. The remaining separation of the tune traces is a direct measure of the total coupling coefficient. In the latter method, a single kick is applied in one plane and the time evolution of the betatron oscillations in both planes observed. Other methods are under study.

## 13.8 APERTURE AND NON-LINEAR MEASUREMENTS

According to simulations, the single particle motion is naturally unstable in the nominal LHC unless some non-linear field harmonics are properly corrected (sextupole to dodecapole). There is therefore a requirement to give access to the beam observables related to the non-linear beam motion to allow deterministic corrections. The measurement principles are sometimes new but more often take advantage of existing ones provided their accuracy can be significantly increased. The methods anticipated for LHC and the requirement they put on the instruments are reviewed below.

### 13.8.1 Measurement of the Dynamic Aperture by the Kick Method

This well-known method may be hazardous at LHC at 7 TeV as the damage limit could be approached or reached, even for a pilot bunch. The non-linear fields localised in the triplets can however be studied by other methods (see Sec. 13.8.7). At 450 GeV, the non-linear fields are diffuse in the whole machine and the kick method appears the most suitable. It was therefore decided to increase the strength of the Q-kickers to allow a maximum oscillation amplitude of  $8\sigma$  at 450 GeV ( $2\sigma$  at 7 TeV) [20] whilst keeping an upgrade at 7 TeV possible. Interlocks on the beam intensity will be provided to prevent too high beam losses that could induce quenches. Combining functionalities in the Q-kickers implies that 25% of the 2808 bunches are deflected at each kick.

### 13.8.2 Measurement of the Dynamic Aperture by the Blow-up Method

This method involves blowing up the beam transversely by successive sweeps through its eigen-frequencies and measuring the cut in the transverse density profile caused by the dynamic aperture. The blow-up can be provided by the LHC damper system driven by an external sweeping or noise source. The dynamic range of the transverse profile monitors is specified to measure 1% of the density provided by a single pilot bunch diluted over the expected aperture with an accuracy of 10% [21].

### 13.8.3 Measurement of the Amplitude Detuning

A single kick to large amplitude will cause 25 % of the beam to oscillate at amplitudes between 0 and  $8\sigma$  at 450 GeV and 0 to  $2\sigma$  at 7 TeV. The bunch-by-bunch Q-meter will be able to directly measure the tunes versus amplitudes. The accuracy will be limited by the de-coherence time rather than the instrument and can be maximised by modern processing techniques, e.g. [22]. Other methods may be contemplated, using coherent oscillations or dc orbit oscillations. With collisions, the tune-spread becomes a more relevant and accessible observable.

### 13.8.4 Measurement of Average $b_5$ Using the Third-order Chromaticity

The dominant non-linear term at injection is  $b_5$ . It originates in the dipoles and must be corrected to better than 20 % by decapole correctors. The beam observable is the third-order chromaticity. A PLL tune-meter with a resolution of  $10^{-5}$  or better is needed [23]. This, however, can be provided with a relatively slow response time (seconds) [24].

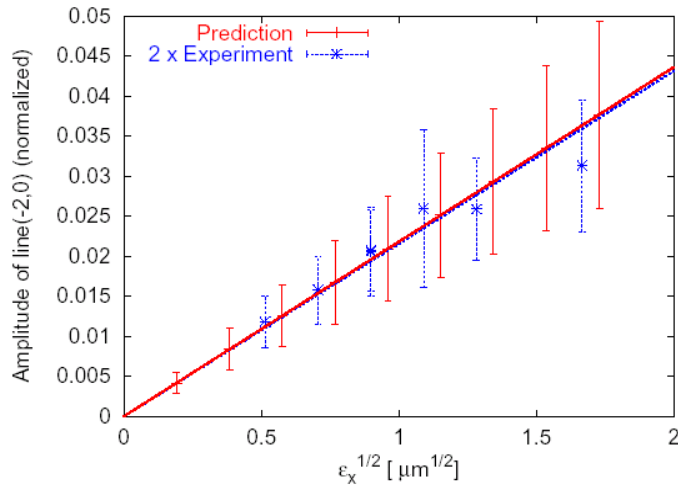


Figure 13.10: Normalized amplitude dependence of the 3Qx driving term [19]

### 13.8.5 Measurement of the Chromatic Coupling Related to $a_3$

The parasitic skew sextupole fields create by feed-down a linear coupling whose strength varies during the synchrotron oscillation, modulating the betatron tunes [25]. The correction will be based on the measurement of linear coupling for different dc momentum offsets.

### 13.8.6 Measurement of the resonance excitation terms

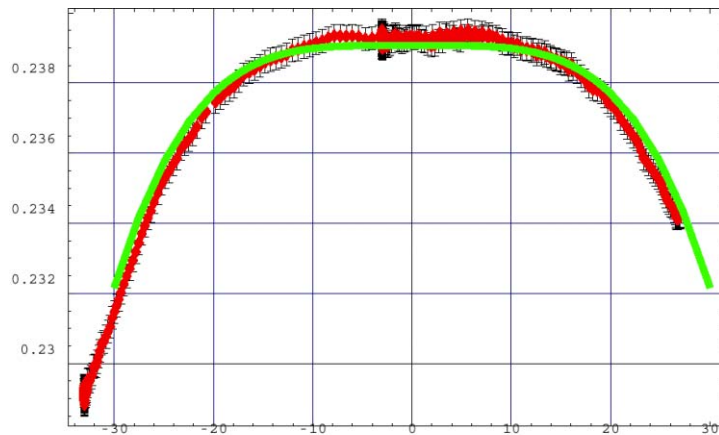


Figure 13.11: Signature of a dodecapole in RHIC. (tune-shift versus bump amplitude [18])

In the presence of non-linearities, the spectrum of the beam oscillation after a kick exhibits harmonics whose strength are related to the dominant resonance driving terms [26]. The method can be implemented in LHC using the Q-kicker as exciter and the turn-by-turn capability of the BPM. The resolution and linearity of the BPM's are consistent with an accurate measurement of third-order resonances. This kick method has the same limitation at 7 TeV (kicker strength, safety) as formerly mentioned.

### 13.8.7 Measurement of the Higher Order Multipoles by Feed-down to the Tunes

The measurement of localised high-order multipoles (or rather action kick) can be made by an accurate measurement of the feed-downs, e.g. the tunes, when applying dc bumps of varying amplitudes at the azimuth of the non-linearity (an example of such a measurement made at RHIC is shown in Fig. 13.11). The method requires a PLL tune meter with a resolution of  $10^{-5}$  or better to detect the highest-order multipole to

be corrected, i.e.  $b_6$  [27]. The anticipated slow time response is perfectly acceptable. The method requires an efficient coordination between instruments and orbit correctors.

### 13.8.8 Measurement of the Frequency Maps

To study the tune diffusion versus oscillation amplitude in the frequency domain, it is necessary to measure the tune to high accuracy ( $10^{-5}$ ) in less than 1000 turns. The method [23] relies on windowing and interpolation in the frequency domain and can take advantage of all BPMs. It has the same constraints as the other kick methods. An example of this type of measurement is shown in Fig. 13.12.

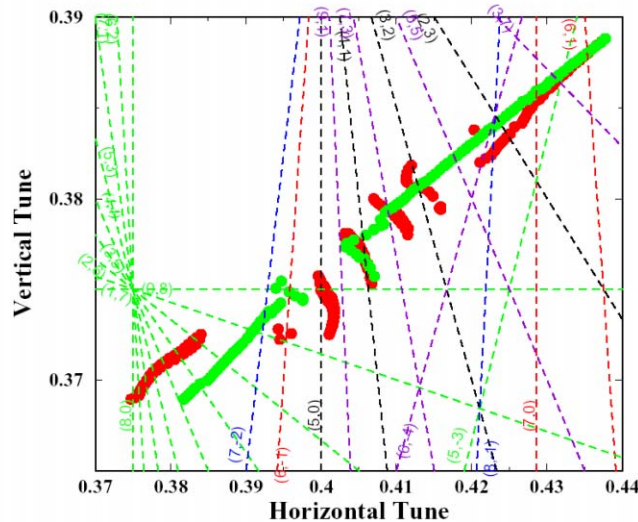


Figure 13.12: Experimental frequency map of the ESRF

### 13.8.9 Measurement of Longitudinal and Transverse Distribution Tails

A consequence of the non-linear motion is the existence of tails of very low densities in the beam distributions. A synchrotron light-based longitudinal profile monitor is planned to provide the longitudinal tails by single-photon counting down to  $10^{-4}$  of the core density [28]. In the transverse plane, a wire-scanner at a steady but controllable position is anticipated to fulfil the requirement of detecting tails down to  $10^{-5}$  of the core density [21].

### 13.8.10 Measurement with an AC Dipole

Recent theoretical studies [29] show the high potential of exciting the beams outside their eigen-frequency spectrum for the measurement of the optics parameters (coupling, de-tuning and resonance driving terms). See Sec. 13.7.2.

## 13.9 OTHER BASELINE INSTRUMENTS / SYSTEMS

### 13.9.1 Dedicated BPMs

The BPMs which do not form part of the main orbit system are listed and briefly described below:

- **BPMC** – a cold BPM located in the Q7-Q10 cryostats in IR4 comprised of a 24 mm button electrode monitor which is used by the orbit system and a 150 mm shorted stripline coupler used by the transverse damper system (Sec. 6.4).
- **BPRS** – a warm, resonant, stripline coupler for PLL tune measurement at IR4 (Sec. 13.7).
- **BPLS** – a warm, long, stripline coupler used for Head-Tail chromaticity measurement in IR4 (Sec. 13.7).
- **BPQS** – a warm, stripline coupler for standard, single kick tune measurement at IR4 (Sec. 13.7).

- BPTX – a 34 mm button electrode monitor (Sec. 13.11) located on the incoming beam at the end of the D2 magnet either side of each of the four main experiments. The BPPTX is used to provide a beam signal to the experiments with which they can verify their trigger timing.
- BPMRF – a warm, stripline coupler located in IR 4 and provided to the RF group for beam diagnostics in the transverse plane.
- Each motorised support used for transverse beam diagnostics (Sec. 13.7) is equipped with a warm, 34 mm button electrode BPM for closed orbit offset compensation.
- The beam dump insertion in point 6 is equipped with four warm, 34 mm button electrode interlock BPMs per ring, intended to ensure that the beam never drifts outside the limited beam dump extraction channel aperture.

### 13.9.2 High Frequency Pickup

The following special pick-ups have been discussed for dedicated studies:

#### *High frequency pick-up*

The purpose of a high frequency pick-up is to detect position and intensity signals for a high band of frequencies ( $\sim 0.5$  to 8 GHz) centred on the cut-off frequency of the LHC vacuum chamber. These pick-ups could be used for the observation of head-tail instabilities. A smooth-response exponential coupler connected via passive hybrid circuits to short, large diameter, air core cables is proposed. The pick-up will be equipped with electrodes in both planes.

#### *Quadrupolar pick-up*

The state of betatron matching at injection can be checked with two such monitors per ring, one where  $\beta_H$  is large and  $\beta_V$  is small and there other where the situation is the other way round. This function is important because emittance conservation in the LHC injection is a critical issue. A quadrupolar pick-up has been developed for the PS but due to the different bunch structure a re-design of the sensor will be necessary.

### 13.9.3 Schottky System

Recent observations from FNAL and BNL indicate that it should be possible to make some basic measurements (tune, momentum spread) at 7 TeV using Schottky pick-ups. It is proposed to use a waveguide structure similar to that tested at FNAL at a frequency around 6 GHz where the width of the transverse sidebands is wide enough to obtain  $10^{-3}$  precision in the tune measurement. At such a high frequency and with sufficient front-end filtering, the observed coherent lines that polluted the Schottky signals in previous stochastic cooling tests should be reduced to a level where the problem is under control and does not lead to head amplifier saturation.

### 13.9.4 Beam Synchronous Timing Receiver

The beam synchronous timing (BST) for the majority LHC beam instrumentation orbit will be distributed via a fibre-optic network, using the Timing, Trigger and Control (TTC) system designed for the LHC detectors [30]. The TTC infrastructure allows the 40 MHz bunch clock, 89  $\mu$ s turn clock and arbitrary control data for each ring to be recuperated at each beam instrumentation station by a BST receiver card (BOBR) [31]. This VME64x card is fitted with either one or two (if timing from both rings are required in the same crate) TTCrm mezzanine cards containing the TTCrx receiver ASIC developed as part of the TTC project [32]. The BOBR has the task of distributing the 40 MHz bunch clock and the 89  $\mu$ s turn clock throughout the VME crate using user defined pins on the P0 connector. In addition the module decodes the message sent on every turn, generating hardware triggers when required or updating software settings. A single command is composed of an 8 bit sub-address and 8-bits of data, allowing up to 256 identified bytes of data to be broadcast. The message transmitted on each turn contains up to 32 such commands, including the machine mode, beam type, beam energy and the GPS absolute time as well as beam instrumentation specific settings and triggers.

## 13.10 NON-BASELINE, STAGED OR PROPOSED INSTRUMENTS

### 13.10.1 Long-Range Beam-Beam Compensation

Due to the small bunch spacing, the LHC beams experience 15 ‘near-misses’ on each side of every collision point. In IP1 and IP5, the beam separation is  $9.5\sigma$  on average. In the other two collision points, the normalised separation is larger and their contribution to the long-range beam-beam effect can be neglected. The non-linear part of the long-range interactions appears to be the dominant mechanism for single particle instability [33], even though the tune spread is small enough (footprint criterion). A very fast diffusion in amplitude is observed for beam amplitudes of 6 to  $8\sigma$ .

The topology of the long-range interactions in LHC makes it possible to devise a simple but accurate weak-strong model where the weak beam, assumed round, is perturbed by currents flowing in wires on either side of the crossing points (strong beam). This model leads naturally to a compensation system [34] made of genuine wires excited by a constant current for the compensation of the normal bunches or by a pulsed current in an option where the PACMAN bunches would be individually corrected.

These wires run along the beam at positions where the beams are already in separate channels. They should be placed between the two channels for a horizontal crossing and above or below for a vertical crossing. The beam-wire distance should be equal to the beam separation at the long-range interaction points ( $9.5\sigma$ ). Studies of robustness show that they can be further retracted to  $12\sigma$ , i.e. well in the shadow of the collimators. The wire excitation is 83 A·m on each side of every crossing point. The  $\beta$ -function is not relevant (provided it is the same in both planes). The phase advance between perturbation and correction must be as small as possible to correct all non-linear terms, not only the detuning. The strong focusing of the LHC low- $\beta$  sections allows suitable positions to be found at 112 m from the crossing points and space has been reserved at them. The phase shift is only  $2.6^\circ$  and the beam channels already sufficiently separated. Numerical simulations [35] show that particles up to  $7\sigma$  are stabilised by the compensation system, i.e. all particles within the collimator acceptance. The robustness of the scheme appears high for all dc effects (errors in excitation and position). The ripple must not exceed 1 per mil to prevent heating the beam.

A 1.25 mm radius (about 1 beam  $\sigma$ ) hollow Cu wire was installed in the SPS to test both the physics and the technology. The wire is brazed on alumina insulators themselves brazed on stainless steel supports. Each of the two devices has an active length of 60 cm. The high current density ( $\sim 100$  A/mm<sup>2</sup>) requires cooling. Water cooling was chosen for the SPS to meet a tight schedule. Purely passive cooling by conduction appears possible and is preferred for LHC, unless super-conducting wires can be used. The onset of strong diffusion in a situation representing the nominal LHC seems now detected [36]. Confirmation will be obtained in 2004 by adding other such devices to compensate the perturbation in a situation close to that of the LHC.

## REFERENCES

- [1] “Measurement of the Beam Position in the LHC Main Rings”, LHC-BPM-ES-0004 v.2 (EDMS Id: 327557), Ext. Ref. Div. SL-BI.
- [2] “The Supply of Button Feedthroughs for the LHC Beam Position Monitors”, LHC-BPM-CI-0004 v.1 (EDMS Id: 108428), Ext. Ref. IT-2530/SL/LHC.
- [3] “Supply of Cryogenic Semi-rigid Coaxial Cables for the LHC Beam Position Monitors”, LHC-BPM-CI-0005 v.1 (EDMS Id: 110698), Ext. Ref. IT-2529/SL/LHC.
- [4] “Technical Specification for the Supply of Feedthrough Assemblies for the LHC Beam Position Monitors”, LHC-BPM-CI-0008 v.1 (EDMS Id 309289), Ext. Ref. CERN - Div. SL.
- [5] D. Cocq, “The Wide Band Normaliser: a New Circuit to Measure Transverse Bunch Position in Accelerators and Colliders”, Nucl. Instrum. Methods Phys. Res., A 416, 1998.
- [6] “Digital Acquisition Board for the LHC Trajectory and Closed Orbit System”, LHC-BI-ES, to be published.
- [7] B. Jeanneret and H. Burkhardt. “Measurements of the Beam Losses in the LHC Ring”, LHC-BLM-ES-0001.00
- [8] B. Dehning, “Beam Instrumentation for Machine Protection”, Proc. of the LHC Performance Workshop, Chamonix XII, CERN-AB-2003-008-ADM.

- [9] A. Arauzo and C. Bovet, "Beam loss detection system in the arcs of the LHC", CERN-SL-2000-052-BI.
- [10] A. Arauzo and B. Dehning, "Configuration of the beam loss monitors for the LHC arcs", LHC Project Note 238.
- [11] R. Jung, et al.: The LHC 450 GeV to 7TeV "Synchrotron Radiation Profile Monitor", CERN-SL-2002-015 BI
- [12] M. Facchini, "Long. Diagnostics Mirror Configuration for the LHC Beam" unpublished
- [13] LHC-B-ES-0005.00 - EDMS 328145
- [14] R. Assmann et al., "Measurement of the relative luminosity at the LHC", LHC-B-ES-0007, CERN, 2003
- [15] E. Gschwendtner, M. Placidi, "Baseline and Requirements for a Luminosity Monitoring at the LHC", to be published.
- [16] J.P. Koutchouk et al., "Excitation of Transverse Beam Oscillations Without Emittance Blow-Up Using The AC-Dipole Principle", Proc. of DIPAC 2001, Grenoble, p.82ff
- [17] F. Bordry, CERN-AB-PO, private communication.
- [18] O.S. Brüning, W. Höfle, R. Jones, T. Linnekar, H. Schmickler, "Chromaticity Measurements via RF Phase Modulation and Continuous Tracking", Proc of 8th European Particle Accelerator Conference, Paris, June 2002, pp 1852-1854.
- [19] R. Jones, H. Schmickler, "The Measurement of Q' and Q" in the CERN-SPS by Head-tail Phase Shift Analysis", Proc. of 2001 Particle Accelerator Conference, Chicago, June 2001, pp 531-533.
- [20] S. Fartoukh et al., Funct. Spec. of the Transverse Measurements, in work, 2003.
- [21] C. Fischer et al., Funct. Spec. of the Transverse Profile Measurements, LHC-B-ES-0006, EDMS328147, 2003.
- [22] J. Laskar, "Frequency Analysis for Multi-Dimensional Systems", Physica D67 (1993) 257-281 & R. Bartolini et al., "Precise Determination of the Betatron Tune", EPAC'96, Sitges, 1996.
- [23] S. Fartoukh, in PLL Workshop, CERN 2002.
- [24] P. Cameron et al., "PLL Tune Measurement during RHIC 2001", EPAC'02, Paris, 2002 & PLL Workshop, CERN 2002.
- [25] J.P. Koutchouk, "Chromatic properties of the LHC lattice", LHC Project Note 113, 1997 & S. Fartoukh, 'Chromatic coupling due to  $a_3$  and correction', LHC Project Report 278, 1998.
- [26] M. Hayes, F. Schmidt, R. Tomas, "Measurement of Resonance Driving Terms at SPS", Proc. of EPAC'02, Paris, 2002.
- [27] F. Pilat et al., "Linear/Nonlinear Corrections in the RHIC Interaction Regions", Proc. of EPAC'02, Paris, 2002.
- [28] C. Fischer et al., Funct. Spec. of the Longitudinal Profile Measurements, LHC-B-ES-0005, EDMS 328145, 2003.
- [29] S. Peggs, PAC'99, New York, 1999. & S. Fartoukh, "Linear Coupling Coefficients via AC dipole excitation", CERN-SL-2002-059 AP, 2002. & R. Tomas, "Normal Form of Particle Motion under the influence of an AC-dipole", Phys. Rev ST Accel. Beams, vol.5 54001 (2002).
- [30] B.G. Taylor, "TTC Distribution for LHC Detectors", IEEE Trans. Nuclear Science, Vol. 45, No. 3, pp. 821-828, 1998.
- [31] "BOBR - The Beam Synchronous Timing Receiver Interface for Beam Observation Systems", LHC-BI-ES, to be published.
- [32] J. Christiansen, A. Marchioro, P. Moreira; "TTCrx: an ASIC for timing, trigger and control distribution in LHC experiments" in 2nd Workshop on Electronics for LHC Experiments, Balatonfüred, Hungary, September 1996, p. 161-165.
- [33] Y. Papaphilippou, F. Zimmermann, "Weak-strong beam-beam simulations for LHC", CERN-SL-99-039 AP, 1999.
- [34] J.P. Koutchouk, "Correction of the Long-Range Beam-beam Effect in LHC", Proc. of IEEE PAC2001, Chicago (2001).
- [35] F. Zimmermann, "Weak-strong simulations studies for the LHC long-range beam-beam compensation", Proc. of beam-beam Workshop, Fermilab, June 2001.
- [36] J.P. Koutchouk, J. Wenninger, F. Zimmermann, in work.